Research Journal of Chemical Sciences ISSN 2231-606X
Vol. **16(1),** 18-23, February **(2026)** *Res. J. Chem. Sci.*

A Study of the Degradation of an Organic Acid Induced by a Photocatalytic Cement-TiO_2-W Nanocomposite

Aniedi E. Nyong*, Clement O. Obadimu, Joseph Alexander, Wisdom George, Godwin J. Udo, Joachim J. Awaka-Ama
Akwa Ibom State University, Department of Chemistry, Physical and Materials Chemistry Unit, P.M.B 1167, Post Code 532111, Ikot Akpaden, Akwa Ibom State, Nigeria
aniedinyong@aksu.edu.ng

Available online at: www.isca.in, www.isca.me
Received 27th September 2025, revised 30th November 2025, accepted 10th January 2026

Abstract

The preparation of the cement nanocomposites involved the physical dispersion of TiO_2 nanoparticles doped with 1-3 wt. % of tungsten (W) within the cement matrix prior to hydration. From the SEM evaluation, the nanoparticles were in the size range of 18 ± 1.25 nm. These cement nanocomposites were used in inducing the photodegradation of stearic acid, on interaction with UV light rated at 8 W, through absorbance and water contact angle measurements. The percent phodegradation efficiency depended on the amount of the nanoparticles incorporated into the cement nanocomposites. In the absorbance studies, the maximum percent photodegradation efficiency of 91 percent was calculated for the cement-6.67wt.% TiO_2-W nanocomposite after exposure to UV light for 2 hours. Lower percentages of the photodegradation efficiency, based on the measured water contact angles, were calculated. A maximum of 84.77% was noted after 6 hours of exposure of the coated cement-6.7wt.% TiO_2-W nanocomposite and at this instant, the contact angle was 18.29°±3.96°. The Langmuir-Hinshelwood model was used in evaluating the velocity constants of the photodegradation of the stearic acid. The velocity constants from this model ranged from 0.80–1.36hr^{-1} for the various cement-TiO_2-W nanocomposite used in the experimentations.

Keywords: Photodegradation, Cement Nanocomposite**,** Stearic Acid, Absorbance, Contact Angle.

Introduction

A particular means of determining the wet ability of surfaces is through contact angle evaluation. The contact angle is the angle a fluid, such as water, oil etc, creates when it is in contact with a solid surface[1,2]. Its value is determined by the properties of the solid surface and those of the liquid as well by the forces existing between the solid and the liquid[3,4]. The Young's equation (1) expresses the contact angle in terms of the interfacial energy, which is a surface property and is the fundamental equation that relates the contact angle of fluids to the solid surface properties:

$$\cos\theta_c = \frac{\gamma_{sg}-\gamma_{sl}}{\gamma_{lg}} \quad (1)$$

where the interfacial energies of the solid-gas, solid-liquid and liquid-gas interfaces are represented by γ_{sg}, γ_{sl} and γ_{lg} respectively.

The contact angle behaviour of surfaces with respect to water and oilis useful in justifying the self-cleaning capability of surfaces[5]. To this end, the surfaces in which the contact angles are above 150° or below 5° are considered as self-cleaning[6,7]. This has become a significant point of technological, environmental and biological interest[8,9]. Therefore, surfaces of materials have been moderated both physically and chemically by addition of nanoparticles and through coating with long-chain fatty acids[10], silanes[11,13], polymers[14] to mention but a few; for them to become self-cleaning or exhibit the so called "lotus effect"[15].

Amongst the nanomaterials that have been used to induce such lotus effect, photocatalytic semi-conductors have been used the most prominent[16,17]. Such semi-conducting nanoparticles convey photocatalytic activity on surfaces through which degradation of water-bound organic matter for self-cleaning is achieved. Extensive researches have been reported in literature, in which numerous kinds of photocatalyst have been studied for their photo-degradation efficiencies[18,19]. Some of these photocatalyst include TiO_2[20], ZnO [21], doped TiO_2[22] etc.

For instance, TiO_2 nanoparticles have been added to cements for them to exhibitself-cleaning capability[23]. Equally gypsum plaster has been modified by TiO_2 and in another case, enriched with glass fiber and was found to have capacity to degrade a certain organic matter[24, 25]. To this end, new technologies have been developed including among others, the technology of photocatalytic coment products, which are capable of exhibiting self cleaning characteristics.

In the light of the above, we have studied the behavior of cement modified with a novel photocatalytic, semi-conducting TiO_2-W nanoparticles. Our intention was to investigate the capacity of this photocatalyst to degrade organic matter and

convey self-cleaning behavior on the cement material. Our approach involved water contact angles as well as absorbance studies. There are no studies presented in literature as at this moment where TiO_2 -W nanoparticles have been investigated for their effect on the self-cleaning and photodegradation capacity of cement-based materials.

Materials and Methods

Materials: The cement that was used for the series of experiments that we carried out was sourced from Lafarge Cement Company of Nigeria. In terms of the chemical composition, the cement consisted of CaO, SiO_2, Al_2O_3 and Fe_2O_3 with the weight percentage of 51.67 ± 3.84, 18.02 ± 0.66, 1.25 ± 0.25 and 10.50 ± 0.76 respectively. The photocatalyst, TiO_2 doped with tungsten (W) was purchased from the company known as US-Nano Research, in the United States of America, and used as received without any further processing. It consisted of the anatase phase of TiO_2 in a weight composition of 97-99 wt.% and tungsten (W) in a weight percentage of 1-3 wt. %. The Stearic acid used in this work was purchased from Sigma-Aldrich, USA while the Ethanol and distilled water were sourced locally in Nigeria. We further constructed a wooden Photo-Reactor consisting of a darkened chamber that had a dimension of 50×40×20 cm, in which a 8.0 W UV light bulb was installed and connected to a power source.

Method: Scanning Electron Microscopy (SEM) was used to evaluate the size of the nanoparticles. This was done at the US Nano Research Laboratory, from which the nanoparticles were obtained. The microscopic evaluation was carried out at a magnification of 10,000x. The cement nanocomposites were prepared through the physical dispersion of the photocatalyst nanoparticles into the Portland cement matrix. This involved dispersion and thorough mixing of known amounts of Portland cement and the TiO_2-W nanoparticles in a ceramic mortar for a fixed time of 10 minutes until both components were properly mixed. The relationship stated in (2) was used in evaluating the weight percentage of the TiO_2-Wnanoparticles needed to generate the cement nanocomposites.

$$\text{Amount of } TiO_2 - W \text{ (in wt. \%)} = \frac{\text{weight of } TiO_2\text{–W (g)}}{\text{Overall weight of cement nanocomposite}} * \frac{100}{1} \quad (2)$$

We set the total weight of the cement nanocomposites to be prepared to 3.0 g. Based on this, the quantities of the TiO_2-W nanoparticles that were added to the Portland cement to generate the samples of the cement nanocomposites were 0.05 g, 0.10 g, 0.15 g and 0.20 g that equated to 1.7 wt. %, 3.3 wt. %, 5.0 wt. % and 6.7 wt.% respectively. This mixture was then hydrated by adding water thecement-TiO_2-W mix at a water to cement/ nanoparticles volume ratio of 1:2. The hydrated cement-TiO_2-W paste were placed indifferent rubber caps that had been lined with thin aluminum foils within. These rubber caps acted as containers in which the samples were allowed to set.

The capacity of the cement-TiO_2-W nanocomposite to photodegrade an organic compound was investigated using absorbance and water contact angle measurements. In the case of the absorbance studies, the samples ofcement-TiO_2-W nanocomposite were immersed in stearic acid solutions (0.02 M), prepared by dissolving 5.6 g of the stearic acid in 1000 ml of ethanol. These were then put inside the darkened chamber of the Photo-reactor and exposed to UV light for120 minutes. Also, other standard solutions of stearic acid were also exposed to the same UV light source for the same time frame of 120 minutes but without the cement-TiO_2-W nanocomposite samples being immersed in these solutions, for the generation of calibration curves. The Helios UV visible spectrophotometer manufactured by Thermostatic Spectronic was used in the absorbance measurements. We set the equipment to operate at the absorption wavelengths of 380 nm and 400 nm for the absorbance studies.

In the measurements of the water contact angles, stearic acid (0.02 M) was used in forming a thin layer of coating on the surfaces of the cement-TiO_2-W nanocomposite samples through a 1 hour dip coating process. After the dip coating, the coated samples were put in a desiccators for them to dry. The coated cement-TiO_2-W nanocomposite samples were then placed in the Photo-reactor and exposed to UV light for 120, 240 and 360minutes respectively. After this, we performed the water contact angles measurements. This involved putting a tiny drop of water on the surfaces of the nanocomposite samples by means of a needle attached to a syringe containing distilled water. The contact angles thereof were measured using the Rame Hart model 250 contact angle goniometer, which operates with the drop image software.

Results and Discussion

We present the results and the discussion for these series of experiments as follows.

Characterization of TiO_2 doped with tungsten (W) nanoparticles: The size determination for the TiO_2-W nanoparticles was through SEM evaluation, seen in Figure-1. This analysis showed that the nanoparticles were roughly spherical in morphology, with the average size of 18 ± 1.25 nm.

Absorbance studies: Based on the Beer-Lambert's law, the absorbance of the various standard solutions of stearic acid were used to prepare calibration curves[26]. The concentrations of the standard solution of stearic acid were in the range of 0.005 M to 0.035 M. The calibration curves were plotted for two absorbance wavelengths (λ) of 380 nm and 400 nm and are presented in Figure-2.

Using these calibration curves, the final concentrations of the 0.02 M stearic acid solutions, in which the various cement-TiO_2-W nanocomposite samples were immersed and exposed to the UV light, were determined. These final concentrations so

determined were $2.7x10^{-3}$ M, $2.2x10^{-3}$ M, $1.7x10^{-3}$ M and $1.5x10^{-3}$ M as well as $3.5x10^{-3}$ M, $3.0x10^{-3}$ M, $2.5x10^{-3}$ M and $1.9x10^{-3}$ M for the samples that were loaded with 1.7 wt.%, 3.3 wt.%, 5.0 wt.% and 6.7 wt.% the TiO_2-W nanoparticles and studied at the absorbance wavelength of 380 nm and 400 nm respectively.

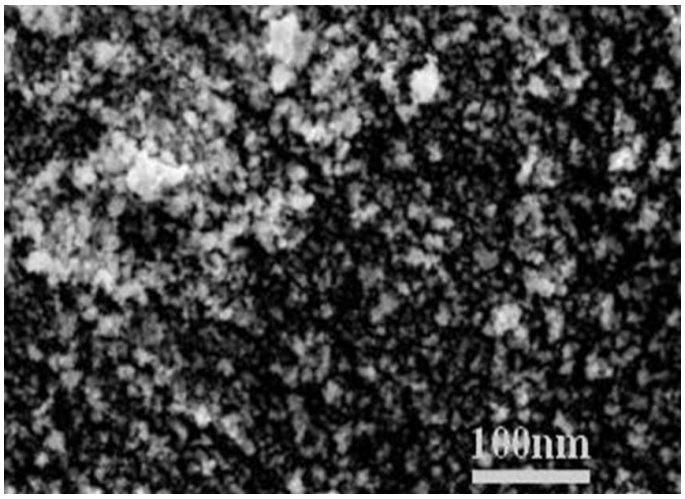

Figure-1: SEM image of TiO_2 doped with tungsten (W) nanoparticles incorporated into cement matrix to produced cement-TiO_2-W nanocomposites.

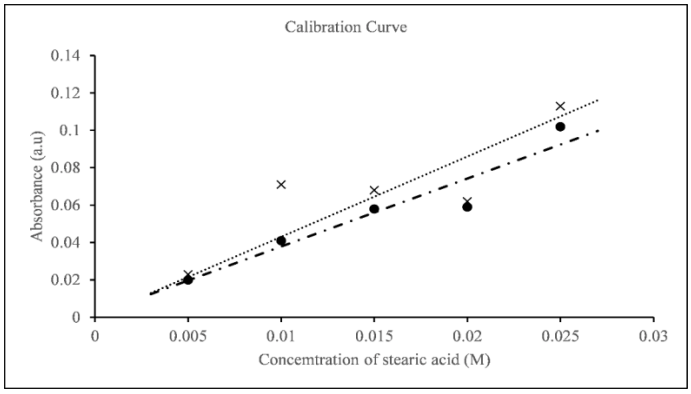

Figure-2: Calibration curves showing the absorbance for the various standard solutions of stearic acids after exposure to UV light for 2 hours.

Water Contact Angle Evaluation: The cement-TiO_2-W nanocomposite samples' surface wet ability was established through the measurement of the contact angles of water, for different durations, prior to and after exposure to UV light. These measured angles are as presented in Table-1.

It was noted that the final concentrations of the stearic acid solutions as well as the water contact angles reduced as the amount of the TiO_2-W nanoparticles in the nanocomposites increased. The angles also reduced as the time of UV light exposure increased. Therefore, these changes are due to the weight percentage composition of the TiO_2-W nanoparticles and the length of the exposure time to the UV light. This is as represented in Figure-3, which shows the changes in the contact angles in terms of the weight percent of TiO_2-W nanoparticles and exposure time of the cement nanocomposite samples.

Table-1: The measured values of water contact angles on surfaces of cement-TiO_2-W nanocomposite samples without and with UV light exposure.

Cement-TiO_2-W nanocomposite samples	Contact angle of water			
	No exposure	2 hours	4 hours	6 hours
Cement-1.7 wt.% -TiO_2/W	123.32 ± 2.65	76.81 ± 3.79	65.11 ± 1.49	40.10 ± 3.11
Cement-3.3 wt.% -TiO_2/W	120.40 ± 1.36	99.33 ± 2.48	62.34 ± 2.86	35.39 ± 1.87
Cement-5.0 wt.% -TiO_2/W	124.55 ± 4.81	82.65 ± 2.85	51.68 ± 1.84	24.91 ± 2.45
Cement-6.7 wt.% -TiO_2/W	120.12 ± 6.14	41.71 ± 2.19	29.53 ± 2.60	18.29 ± 3.96

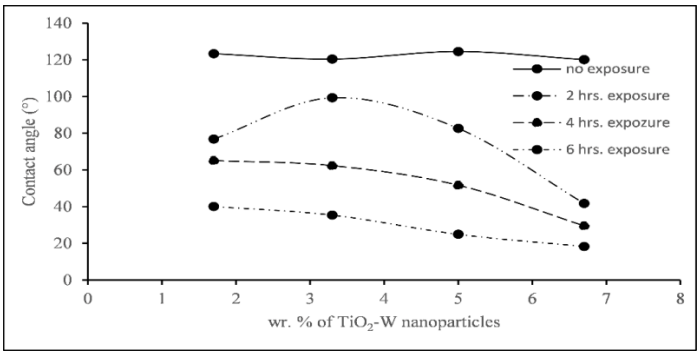

Figure-3: Graph showing the changes in the contact angles of water for the various nanocomposite samples containing various amounts ofTiO_2-W nanoparticles.

Discussion: From the results presented above, there was a reduction in the stearic acid concentration. Furthermore, there was also noticeable reduction in the water contact angles. It should be noted that the roughness of the surface due to heterogeneities present on them as well as the surface energies of the cement-TiO_2-W nanocomposite samples influenced the water contact angles[27]. The decrease in the contact angles is attributable to the surface roughness due to the surface heterogeneities as well as the changes in the surface energies of the samples[28]. Prior to the exposure of the cement-TiO_2-W nanocomposite samples, high contact angles of water were noted, but these values dropped when the samples interacted with the UV source for the various time durations as presented in Figure-3.

The principal reason we adduce for this behavior is the change in the surface energy of the cement samples because of the impact of the degradation of the stearic acid surface coating via photocatalysis. This photodegradation followed the interaction

of the ultra-violet light with TiO_2-W nanoparticles, present within the matrices of the cement nanocomposites, by which holes (h^+) and electrons (e^-) are generated. It has been established that the use of tungsten (W) as dopant ensures the release of two electrons for every one tungsten atom[29,30]. This implies that the low quantities of the tungsten used in doping TiO_2 induced photocatalytic behaviors, in combination with the TiO_2, in the cement nanocomposite samples.

Furthermore, the expected photodegradation pathway involved the conversion, by positively charged holes (h^+), of the H_2O molecules found in the solution as well as in the coated layers of stearic acid to hydrogen (H^+) ions and hydroxyl (OH^-) free radicals[31]. The hydroxyl free radicals generated by means of these holes in the photocatalyst furthered the photodegradation by reacting with O_2 molecules restrained within the stearic acid coating and in its solution. This causes the further production of more hydroxyl free radicals to continue the photodegradation process[32].

Thus, by increasing the weight percent of the TiO_2-W nanoparticles in the nanocomposites, the inclination towards the generation of the OH^-ions, photochemically, increased. It is due to this that there is a further reduction in the contact-angles as well as in the stearic acid's final concentrations, as noted from the absorbance experiments. The decrease in both the stearic acid concentration and in the contact angles were consistent at all the weight percentages of theTiO_2-W nanoparticles loaded into the cement nanocomposite matrices.

Evaluation of Photodegradation efficiency: We calculated the photodegradation efficiencies of the cement-TiO_2-W nanocomposites through the results obtained from the absorbance studies and from the water contact angles measurements. The relationships stated below were used in calculating the values of the percent photodegradation efficiency, based on the absorbance studies (3) and contact angle measurements (4):

$$\% E = \frac{C_o - C_T}{C_o} * 100 \quad (3)$$

$$\% E = \frac{\theta_o - \theta_T}{\theta_o} * 100 \quad (4)$$

In equation (3), C_o and C_T represent the initial and final stearic acid concentrations for the solutions containing the different cement-TiO_2-W nanocomposite samples, before and after their interaction with the UV light. In the same vein in equation 4, Θ_o and Θ_T represents the water contact angles measured on the surfaces of the cement-TiO_2-W nanocomposite samples before and after their interactions for a specific period with the UV light.

The calculated photodegradation efficiencies (% E) based on equation 3 were 85.5%, 87.5%, 91% and 93.5% as well as 80%, 84.5%, 86.5% and 91%, from UV spectrophotometric examinations carried out at 350 nm and 400 nm respectively; for the 0.02 M stearic acid solutions containing cement-TiO_2-W nanocomposite samples loaded with 1.7 wt.%, 3.3 wt. %, 5.0 wt. % and 6.7 wt.% of TiO_2-W nanoparticles respectively. However from equation 4, the calculated photodegradation efficiencies (%E) were 37.71%, 42.20%, 67.48%; 17.5%, 48.22%, 70.61; 33.64%, 58.50%, 80% and 65.28%, 75.41%, 84.77% from the contact angles of water measured on the stearic acid coated surfaces of the cement nanocomposites loaded with 1.7 wt.%, 3.3 wt.%, 5.0 wt.% and 6.7 wt.% of TiO_2-W nanoparticles and exposed to 2-,4- and 6-hours of UV light respectively. The values for the photodegradation efficiencies were much lower, from the results obtained from the contact angle of water measurement when compared to those obtained from the absorbance studies. This can be adduced to the very limited amount of water molecules trapped with the thin layer coating which is necessary in initiate the formation of the hydroxyl ions that is important in the photodegradation process.

Examination of the Photodegradation Kinetics: In several scientific investigations, the Photodegradation Kinetics of various organic compounds is investigated using the Langmuir-Hinshelwood model[33]. In this model, the variation in the concentrations of organic compounds as a function of time is studied with some specific assumptions. These assumptions include the consideration that the surfaces of the photocatalytic materials are heterogeneous in nature and with a specific number of sites available for chemisorption[34]. The Langmuir-Hinshelwood model is given in equation 5,

$$In\frac{C_T}{C_o} = -K_1 t \quad (5)$$

where $K_1$is the rate constant for a pseudo first-order reaction kinetics and t is the time. Considering the time in which the absorbance study was carried out, the pseudo-first-order rate constants was calculated and are presented in Table 2 for the variousCement-TiO_2-W nanocomposite samples.

Table-2: Values of K_1 estimated from Langmuir-Hinshelwood model from absorbance studies at λ = 380 nm and 400 nm.

Cement-TiO_2-W nanocomposite samples	Rate Constant, (K_1) hr^{-1}	
	380 nm	400 nm
Cement-1.67 wt.% (TiO_2-W) nanocomposite	0.97	0.80
Cement-3.33 wt.% (TiO_2-W) nanocomposite	1.04	0.93
Cement-5.00 wt.% (TiO_2-W) nanocomposite	1.20	1.00
Cement-6.67 wt.% (TiO_2-W) nanocomposite	1.36	1.20

The K_1 values were found to increase with increase in the amount of the TiO_2-W nanoparticles incorporated into the cement matrices of the nanocomposites. Therefore, by simply

increasing of amount of the nanoparticles resulted in the UV light causing a proportionate increment in the number of holes and electrons that caused the furtherance of the photodegradation process.

Conclusion

From our absorbance and water contact angle studies, we have established that phot-degradation of stearic acid that is in contact with TiO_2-W photocatalyst bearing cement nanocomposites, is possible under low intensity UV irradiation. The changes concentrations of the stearic acid as well as in the contact angles of water was used to determine the percent photodegradation efficiencies. The photodegradation efficiencies increased with increase in the weight percent of the TiO_2-W nanocomposites incorporated into the nanocomposites. Furthermore, the kinetics of the photodegradation was appraised effectively through both the absorbance. On the basis of a pseudo-first-order kinetics and using the Langmuir-Hinshelwood model, the rate constants for the photodegradation of the stearic acid were calculated. The values of the rate constant, K_1, obtained from the Langmuir-Hinshelwood model were higher as the weight percent composition of the TiO_2-W nanoparticles increased in the nanocomposite samples at both 380 nm and 400 nm, of exposure to the UV irradiation source. To this end, it was noted that the rate constants increased with increase in the amount of TiO_2-W photocatalyst present in the cement nanocomposite.

References

1. Wu Y., Dong L., Shu X., Yang Y., She W. & Ran Q. (2022). A review on recent advances in the fabrication and evaluation of superhydrophobic concrete. *Compos B Eng*., 237, 109867.

2. Huhtamäki T., Tian X., Korhonen J. T. & Ras R. H. A. (2018). Surface-wetting characterization using contact-angle measurements. *Nat. Protoc.*, 3, 1521–1538. https://doi.org/10.1038/s41596-018-0003-z.

3. Nyong A., Peter I., Awaka-Ama J. & Udoh G. (2021). Self-Cleaning Materials: Review of Recent Progress and Innovations. *Researchers Journal of Science and Technology*, 1(1),64-71.

4. Marmur A., Volpe C. D., Siboni S., Amirfazli A. & Drelich J. W. (2017). Contact angles and wet ability: towards common and accurate terminology. *Surf Innov.*, 5(1), 3–8. https://doi.org/10.1680/jsuin.17.00002.

5. Drelich J. W. (2019). Contact angles: From past mistakes to new developments through liquid-solid adhesion measurement*s*. *Adv. Colloid Interface Sci.*, 267, 1-14. https://doi.org/10.1016/j.cis.2019.02.002.

6. Reevahan J., Chandrasekaran M., Joseph B. G., Durairaj R. B. & Mageshwaran G. (2018). Superhydrophobic surfaces: A review on fundamentals, applications, and challenges. *J. Coat. Technol. Res.*, 15, 231–250. https://doi.org/10.1007/s11998-017-0011-x.

7. Liu W., Wang X., Xiang S., Lian Y. & Tao S. (2024). Stretchable Superhydrophobic Surfaces: From Basic Fabrication Strategies to Applications. *Processes*., 12(1), 1-48. https://doi.org/10.3390/pr12010124.

8. Xu Q., Zhang W., Dong C., Sreeprasad T. S. & Xia Z. (2016). Biomimetic self-cleaning surfaces: synthesis. Mechanism and applications,. *J. R. Soc. Interface.*, 22, 20160300. https://doi.org/10.1098/rsif.2016.0300.

9. Prathapan R., Venkatesan A. G., Nair S. & Nair S. (2014). A review on 'self-cleaning and multifunctional materials. *J. Mater. Chem. A.*, 2, 14773–14797. https://doi.org/10.1039/C4TA02542C.

10. Nyong A. E., Udoh G. J., Awaka-Ama J. J., Effiong J. F., Ekwere I., Obadimu C. & Rohatgi P. (2023). Cu-32.02% Zn-2.30% Pb alloy surface superhydrophobicity induced by an arachidate layer. *Acad. mater. Sci*., 1(1), 1-7. https://doi.org/10.20935/AcadMatSci6138.

11. Nie Y., Ma S., Tian M., Zhang Q., Huang J., Cao M., Li Y., Sun L., Pan J., Wang Y., Bi P., Xu H., Zeng J., Wang& Xia Y. (2021). Superhydrophobic silane-based surface coatings on metal surface with nanoparticles hybridization to enhance anticorrosion efficiency, wearing resistance and antimicrobial ability. *Surf. Coat. Technol.*, 410 (126966), 1-11.

12. Zhang L., Zhou A. G., Sun B. R., Chen K. S.& Yu H. (2021). Functional and versatile superhydrophobic coatings via stoichiometric silanization. *Nat. Commun*., 12 (982), 1-7. https://doi.org/10.1038/s41467-021-21219-y.

13. Qian H., Lu C., Huang J., Luo Z., Wang H., Hou Z., Wang C., Li L., Gao Q. & Zhu M. (2024). Fabrication of a silane-modified superhydrophobic TiO_2–PVDF–FEP coating with scale inhibition performance. *Front. Mater. Sci.*, 18(4), 1-10. https://doi.org/10.1007/ s11706-024-0707-7.

14. Ganesh V. A., Raut H. K. & Nair S. A., Ramakrishna S. (2011). A review on self-cleaning coatings. *J. Mater. Chem.*, 21(41), 16304-16322. https://doi.org/10.1039/ C1JM12523K.

15. Yamamoto M., Nishikawa N., Mayama H., Nonomura Y., Yokojima S., Nakamura S.& Uchida K. (2015). Theoretical Explanation of the Lotus Effect: Superhydrophobic Property Changes by Removal of Nanostructures from the Surface of a Lotus Leaf. *Langmuir*, 31(26), 7355–7363. https://doi.org/10.1021/acs. langmuir.5b00670.

16. Yu C., Sasic S., Liu K., Salameh S., Ras R. H. A. & Ommen J. R. (2020). Nature–Inspired self–cleaning surfaces: Mechanisms, modelling, and manufacturing. *Chem. Eng. Res. Des.*, 155, 48–65. https://doi.org/10.1016/ j.cherd.2019. 11.038.

17. Nyong A. E., Udoh G., Awaka-Ama J. J., Nsi E. W.& Rohatgi P. K. (2022). A study of themorphological changes and the growth kinetics of the oxides formed by the high temperature oxidation of Cu-32.02% Zn-2.30% Pb Brass. *Mater. Res*., 25, 1-6. https://doi.org/10.1590/1980-5373-MR-2021-0173.

18. Chakravorty A., Roy S. (2024). A review of photocatalysis, basic principles, processes, and materials. *Sustainable Chemistry for the Environment*, 8 (100155), 1-18. https://doi.org/10.1016/j.scenv.2024.100155.

19. Effiong J. F., Nyong A. E., Boekom E. J.& Simon N. (2023). Photocatalytic Degradation and Kinetics of Dyes in Textile Effluent Using UV–ZnO-Al System. *Asian J. Appl. Chem.,* 13 (2), 23-32. http//doi: 10.9734/ajacr/2023/v13i2240.

20. Effiong J. F., Nyong A. E., Udoh G. & Obadimu C. (2023). Photocatalytic degradation and kinetics of dyesin textile effluent using UV-TiO_2-W system. *J. Mater. Environ. Sci.*, 14(8), 935-946.

21. Effiong J. F., Boekom E. J., Simon N. & Nyong A. E. (2023). Effect of ZnO Nanoparticles on the Kinetics and Photo-degradation of certain Textile Effluent Dye. *Asian J. Appl. Chem.*, 14(2), 56-64. http//doi: 10.9734/ajacr/2023/v14i2264.

22. Khlyustova A., Sirotkin N., Kusova T.& Kraev A., Titov V., Agafonov A. (2020). Doped TiO_2: the effect of doping elements on photocatalytic activity. *Mater. Adv.,* 1(5), 1193-1201. https://doi.org/10.1039/D0MA00171F.

23. Pietrzak A., Adamus J. & Langier B. (2016). Application of Titanium Dioxide in Cement and Concrete Technology. *Key Eng. Mater*., 687, 243-249. https://doi.org/10.4028/www.scientific.net/KEM.687.243.

24. Janus M., Bubacz K., Zatorska J., Kusiak-Nejman E., Czyzewski A. & Morawski A. (2015). Preliminary studies of photocatalytic activity of gypsum plasters containing TiO_2 co-modified with nitrogen and carbon. *Pol. J. Chem. Technol.,* 17(2), 96-102.https://doi.org/10.1515/pjct-2015-0036.

25. Zając K., Janus M. & Morawski A. W. (2019). Improved Self-Cleaning Properties of Photocatalytic Gypsum Plaster Enriched with Glass Fiber. *Materials (Basel)*, 12(3), 1-15. https://doi.org/10.3390/ma12030357.

26. Swinehart D. F. (1962). The Beer-Lambert Law. *J. Chem. Educ.*, 39(7), 333–336. http//doi:10.1021/ED0 39P333.

27. Guo Z., Hakkou R., Yang J. &Wang Y. (2021). Effects of surface heterogeneities on wetting and contact line dynamics as observed with the captive bubble technique. *Colloids Surf. A Physicochem. Eng. Asp.*, 615 (126041), 1-8. https://doi.org/10.1016/j.colsurfa.2020.126041

28. Palencia M. (2017). Surface free energy of solids by contact angle measurements. *J. sci. technol. appl.*, 2(17), 84-93. https://doi.jsta.cl/resource?doi=j.jsta.17.2.17.

29. Chen D., Xu G., Miao L., Chen L., Nakao S.& Jin P. (2010). W-doped anatase TiO_2 transparent conductive oxide films: Theory and experiment. *J. Appl. Phys.*, 107,063707-1-063707-4.https://doi.org/10.1063/1.3326940.

30. Couselo N., García Einschlag F. S, Candal R. J.&Jobbágy M. (2008). Tungsten-Doped TiO_2 vs Pure TiO_2 Photocatalysts: Effects on Photobleaching Kinetics and Mechanism. *J. Phys. Chem. C*, 112, 1094–1100. https://doi.org/10.1021/jp0769781.

31. Fujishima A., Rao T. N. & Tryk D. A. (2020). Titanium Dioxide Photocatalysis. *J. Photochem. Photobiol. C: Photochem. Rev.*, 1, 1-21. https://doi.org/10.1016/S1389-5567(00)00002-2.

32. Cho M., Chung H., Choi W. & Yoon J. (2024). Linear correlation between inactivation of E. coli and OH radical concentration in TiO_2 photocatalytic disinfection. *Water Res.*, 38(4), 1069-1077. https://doi.org/10.1016/j.watres. 2003.10.029.

33. Vasanth K. K., Porkodi K. & Rocha F. (2008). Langmuir–Hinshelwood kinetics – A theoretical study. *Catal. Commun.*, 9, 82-84. https://doi.org/10.1016/j.catcom. 2007.05.019.

34. Sun N.,Si X., He L., Zhang J. & Sun Y. (2024). Strategies for enhancing the photocatalytic activity of semiconductors. *Int. J. Hydrogen Energy.* 58, 1249-1265. https://doi.org/10.1016/j.ijhydene.2024.01.319.